·临床研究·

广州市某三甲医院不同来源鲍曼不动杆菌的比较基因组学分析

李　康[1]，杨艳鲜[2]，吴昌哺[3]，邵　莉[1]，钟兰兰[3]，陈定强[4]，田国宝[3]
（1. 西藏民族大学医学院，陕西 咸阳 712099；2. 中山大学附属第五医院药学部，广东 珠海 519000；3. 中山大学医学院，广东 深圳 518107；4. 南方医科大学珠江医院检验医学部，广东 广州 510280）

摘　要：【目的】比较广州市某三甲医院临床感染来源与医院环境来源鲍曼不动杆菌（AB）在分子流行病学特征、耐药性、消毒剂耐受性、毒力及相关基因分布、质粒流行特征等方面的差异，评估环境菌株与临床菌株的关联性及环境污染的潜在传播风险。【方法】收集 2024—2025 年广州市某三甲医院 118 株临床来源及 102 株医院环境来源的 AB。采用质谱及 16S rRNA 测序鉴定菌种；琼脂稀释法测定 8 种抗菌药物的最小抑菌浓度（MIC）；结晶紫染色法评估生物膜形成能力；大蜡螟感染模型评价菌株毒力；通过全基因组测序进行多位点序列分型（MLST）、系统发育分析、耐药、耐消毒剂和毒力基因分布并进行质粒筛选。【结果】220 株 AB 共鉴定出 38 种已知 ST 型，以 ST2 和 ST40 为优势谱系。药敏试验显示，临床感染组对米诺环素（MC）、亚胺培南（IMP）等抗生素的耐药水平，以及三氯生（TCS）和苯扎溴铵（BAB）消毒剂的耐受水平均普遍高于环境来源组（$P<0.001$），且 bla_{OXA-23}、*adeB* 等耐药基因检出率均超过 70.0%。统计学评价证实，TCS 与 BAB 的 MIC 值同多种抗生素耐药表型呈显著正相关（$P<0.05$）。生物膜实验中，环境来源组中强成膜菌株的比例（64.7%）显著高于临床感染组（11.9%；$\chi^2=69.06$，$df=2$，$P<0.000\ 1$），且菌株致死率随成膜能力增强而提高。此外，共检出 41 个质粒谱系及 219 种插入序列（IS），IS1006 及 IS1007 等 IS 与 bla_{OXA-23} 及 *katA* 等耐药、毒力基因存在高频共现。【结论】该三甲医院 AB 的优势谱系为 ST2 与 ST40。临床感染组的抗生素耐药性和消毒剂的耐受水平普遍高于环境来源组，环境来源组强生物膜形成能力更突出，临床感染组则以弱的优化及多重耐药菌的分子流行病学监测提供参考。

关键词：鲍曼不动杆菌；分子流行病学；耐药；毒力；消毒剂耐受
中图分类号：R378　　**文献标志码：**A　　**文章编号：**1672-3554（2026）03-0518-10
DOI：10.11714/jsysu.med.YX20260046

Comparative Genomic Analysis of *Acinetobacter Baumannii* from Different Sources in a Tertiary Hospital in Guangzhou

LI Kang[1], YANG Yanxian[2], WU Changbu[3], SHAO Li[1], ZHONG Lanlan[3], CHEN Dingqiang[4], TIAN Guobao[3]
(1. School of Medicine, Xizang Minzu University, Xianyang 712099, China; 2. Department of Pharmacy, The Fifth Affiliated Hospital of Sun Yat-sen University, Zhuhai 519000, China; 3. School of Medicine, Sun Yat-sen University, Shenzhen 518107, China; 4. Division of Laboratory Medicine, Zhujiang Hospital, Southern Medical University, Guangzhou 510280, China)
Correspondence to: TIAN Guobao; E-mail: tiangb@mail.sysu.edu.cn

Abstract:【Objective】To compare the differences between clinical and environmental sources of *Acinetobacter baumannii* (AB) at a tertiary hospital in Guangzhou in terms of molecular epidemiological characteristics, antimicrobial resistance, disinfectant tolerance, virulence and the distribution of related genes, as well as plasmid epidemiological characteristics; and to assess the association between environmental and clinical strains and the potential transmission

收稿日期：2026-03-20　　**录用日期：**2026-04-27
基金项目：国家自然科学基金青年科学基金（82325033）
作者简介：李康，第一作者，E-mail：459506791@qq.com；田国宝，通信作者，教授，研究方向：抗生素耐药性，E-mail：tiangb@mail.sysu.edu.cn

risks associated with environmental contamination.【Methods】A total of 118 clinical and 102 environmental AB isolates were collected from a tertiary hospital in Guangzhou between 2024 and 2025. Species identification was performed using mass spectrometry and 16S rRNA sequencing; minimum inhibitory concentrations (MICs) for eight antimicrobial agents were determined using the agar dilution method; biofilm formation capacity was assessed using the crystal violet staining method; A *Galleria mellonella* infection model was used to evaluate the virulence; whole-genome sequencing was employed for multilocus sequence typing (MLST), phylogenetic analysis, and studies on the distribution of resistance, disinfectant resistance and virulence genes, and plasmid screening.【Results】A total of 38 known ST types were identified among the 220 AB strains, with ST2 and ST40 being the predominant lineages. Antimicrobial susceptibility testing revealed that the clinical infection group exhibited resistance to minocycline, imipenem and other antibiotics, as well as the tolerance levels to the disinfectants triclosan and benzalkonium bromide, were generally higher than those in the environmental group ($P<0.001$), and the detection rates of drug resistance genes such as bla_{OXA-23} and *adeB* all exceeded 70.0%. Statistical analysis confirmed that the MIC values of TCS and BAB were significantly positively correlated with various antibiotic resistance phenotypes ($P<0.05$). In biofilm experiments, the proportion of strong biofilm-forming strains in the environmental group (64.7%) was significantly higher than that in the clinical infection group (11.9%; $\chi^2=69.06$, $df=2$, $P<0.000\,1$), and the mortality rate of the strains increased with enhanced biofilm-forming ability. Furthermore, a total of 41 plasmid lineages and 219 insertion sequences were detected; ISs such as IS1006 and IS1007 were frequently co-occurring with resistance and virulence genes including bla_{OXA-23} and *katA*.【Conclusions】The predominant lineages of AB in this tertiary hospital were ST2 and ST40. The clinical infection group generally exhibits higher levels of antibiotic resistance and tolerance to disinfectants compared to the environmental group, while biofilm-forming ability differs : the environmental group dominates in strong biofilm formation, and the clinical group dominates in weak to moderate biofilm formation. Plasmids and ISs may be involved in the co-occurrence and dissemination control strategies and for the molecular epidemiological surveillance of multidrug-resistant bacteria.

Key words: *Acinetobacter baumannii*; molecular epidemiology; antimicrobial resistance; virulence; disinfectant tolerance

[J SUN Yat-sen Univ(Med Sci),2026,47(3):518-527]

鲍曼不动杆菌(*Acinetobacter baumannii*,AB)是一种重要的革兰氏阴性条件致病菌,广泛定植于医院环境及医疗设备,是引起呼吸机相关性肺炎和菌血症等重症感染的主要病原菌[1-2],已被世界卫生组织列为关键病原体之一[3],尤其在ICU等高危科室,其感染显著提高了患者的病死率[4-5]。在抗菌药物与消毒剂的双重选择压力下,AB通过基因突变及水平基因转移不断进化,形成了以ST2为优势克隆的多重耐药谱系[6-7]。AB具有卓越的干燥耐受能力,可在医院环境表面(如床栏、监护仪、呼吸机等)长期存活,形成持续存在的病原体储库[8]。已有研究表明环境分离株与临床感染株具有高度同源性,提示医院环境是AB在患者间传播的关键媒介[9]。当前,国内外研究虽已证实临床来源与环境来源菌株间存在同源性,但两者在耐药表型、消毒剂耐受水平及毒力特征上的具体差异仍需进一步探索[10]。此外,耐药基因、毒力因子及耐消毒剂基因在遗传元件上的共现关系及其表型相关性仍有待系统性解析[11]。本研究通过对某三甲医院220株AB进行全基因组测序与表型分析,对比临床与环境来源组菌株的流行病学特征、耐药及毒力差异,并分析遗传元件与耐药基因的关联性,旨在阐明临床与环境来源组AB的差异及其传播风险,为制定精准防控指南提供依据。

1　材料与方法

1.1　样本来源

共纳入220株AB,包括118株临床菌株、102株医院环境分离菌株。临床菌株收集自2024年8月24日至2025年5月28日广州某三甲医院住院患者送检的临床感染样本,环境菌株来源于2025年3月4日至2025年8月5日该院每2周1次的定期环境监测采样。

本研究收集的临床分离鲍曼不动杆菌来源于常规诊疗过程中的剩余标本,不涉及患者个人身份信息。研究方案已获得医学伦理委员会批准(批准号:2023-KY-016-02)。

1.2 样本分离及培养

所有分离株经麦康凯平板分离纯化后,采用基质辅助激光解吸电离飞行时间质谱(布鲁克公司,德国)进行初步鉴定,并结合16S rRNA基因测序进行菌种确认。测序结果通过NCBI官网BLASTN进行在线比对,与参考序列相似性≥99%者被判定为AB。所有确认为AB的菌株均置于-80 ℃超低温冰箱保存备用。

1.3 药敏试验

采用琼脂稀释法测定多黏菌素B(Polymyxin B, PB)、米诺环素(Minocycline, MC)、亚胺培南(Imipenem, IMP)、妥布霉素(Tobramycin, TOB)、左氧氟沙星(Levofloxacin, LVX)、头孢他啶(Ceftazidime, CAZ)、替加环素(Tigecycline, TGC)、舒巴坦(Sulbactam, SUL)对分离菌株的最小抑菌浓度(minimum inhibitory concentration, MIC)。药敏结果判定参照美国临床和实验室标准化委员会(Clinical and Laboratory Standards Institute, CLSI) M100(2026年版)标准[12]。根据该标准,各药物的耐药折点分别为:PB ≥4 μg/mL、MC ≥4 μg/mL、IMP ≥8 μg/mL、TOB ≥8 μg/mL、LVX ≥8 μg/mL、CAZ ≥32 μg/mL、SUL ≥16 μg/mL。对于TGC,因CLSI尚未建立针对鲍曼不动杆菌的折点,本研究参考美国食品和药物管理局为肠杆菌科设定的折点:MIC ≤2 μg/mL判定为敏感,MIC =4 μg/mL判定为中介,MIC ≥8 μg/mL判定为耐药。该过程使用大肠埃希菌ATCC 25922作为质控菌株。

同时,采用相同方法测定消毒剂三氯生(Triclosan, TCS)和苯扎溴铵(Benzalkonium bromide, BAB)对分离菌株的MIC值,但由于目前尚无CLSI关于消毒剂的药敏判断标准,其结果以MIC值分布形式呈现。该过程使用大肠埃希菌ATCC 25922作为质控菌株。

1.4 生物膜测定

采用结晶紫染色法测定。将复苏菌株配制成0.5麦氏浊度菌悬液,按1∶100比例使用LB液体培养基稀释,接种至96孔板(每孔200 μL,每株设3个平行孔),并设无菌LB对照。37 ℃静置培养48 h。随后用PBS缓冲液洗涤3次,晾干后加体积分数99.5%甲醇固定20 min,生理盐水冲洗,1%结晶紫染色15 min。弃染液,蒸馏水洗至无色,晾干加无水乙醇溶解结晶紫[13]。采用酶标仪测定570 nm吸光度(OD_{570})。以阴性对照OD_{570}均值(AC)为基准,计算待测菌平均值(A)。判定标准:AC<A≤2AC为弱;2AC<A≤4AC为中等;A>4AC为强。

1.5 大蜡螟感染模型

采用大蜡螟幼虫模型评估菌株致病性。分层选取18株不同来源及成膜能力的菌株作为测试组,以标准株ATCC 19606及ATCC 17978作为参考株,同时设PBS对照组与空白对照组。将过夜培养的菌株经离心洗涤(4 000×*g*,室温离心5 min),调整OD_{600}至0.5,经涂板计数后以PBS稀释至1×10^7/μL作为感染工作液。选取体重均匀(约250~300 mg)且活力良好的幼虫,随机分为10只/组。实验组每只注射10 μL感染工作液(感染剂量为1×10^8 CFU),对照组注射同体积PBS或不作处理,于37 ℃培养72 h。每隔12 h观察并记录幼虫死亡情况(以体表变黑且对机械刺激无反应判定为死亡)。采用Kaplan-Meier法绘制生存曲线,并进行Log-rank检验。实验独立重复2次[14]。

1.6 全基因组测序及分析

220株AB在实验室完成基因组DNA提取后,由诺禾致源公司进行全基因组二代测序。加入32株来源于NCBI数据库的AB参考基因组(见表1)作为参考序列,原始数据经质控、组装后,使用ResFinder数据库进行耐药基因注释,使用VFDB数据库进行毒力基因注释;使用BacMet2 EXP数据库进行耐消毒剂基因注释[15]。

利用MLST 2.23.0软件进行多位点序列分型(multilocus sequence typing, MLST),并使用Kaptive软件进行菌株荚膜多糖(K-locus, KL)和外核心脂多糖(OC-locus, OCL)位点分型鉴定[16]。采用IQ-TREE构建初始最大似然系统发育树,并使用ClonalFrameML识别并去除重组序列[17]。所有系统发育树与基因分布特征通过iTOL平台可视化。

1.7 质粒组学与插入序列分析

基于Tobin等[18]建立的Acinetobacter属质粒数据库,使用ABRicate进行质粒谱系鉴定;提取质粒相关contigs,经MAFFT v7.505比对后采用FastTree v2.1.11构建质粒系统发育树。针对插入序列(insertion sequence, IS),以ISfinder数据库构建BLAST蛋白数据库,通过BLASTp(相似度≥80%、对

表1　纳入鲍曼不动杆菌的参考基因组及来源

Table 1　Reference genomes and source of include *A. baumannii*

Genome accession	Isolation source	Genome accession	Isolation source
GCA_031 197 715.1	Clinical（Blood）	GCF_009035845.1	Urine
GCF_030188385.1	Environmental（Environment）	GCF_000069245.1	Environmental（NA）
GCF_035022445.1	Environmental（Bed）	GCF_040495255.1	Clinical（Urine）
GCF_028550495.1	Pleural effusion	GCF_012272715.1	Clinical（Bronchoalveolar lavage fluid）
GCF_002504145.1	Clinical（Sputum）	GCF_033194575.1	Environmental（NA）
GCF_000021245.2	Environmental（NA）	GCF_007197865.1	Clinical（Bloodstream）
GCF_030551135.1	Clinical（Tracheal secretion）	GCF_031581865.1	Environmental（Broth）
GCF_003994455.1	Clinical（Feces）	GCF_023061375.1	Clinical（Sputum）
GCF_005784945.1	Clinical（Blood）	GCF_029990985.1	Clinical（Pus）
GCA_030486245.1	Clinical（Rectal）	GCA_040948205.1	Clinical（Sputum）
GCA_027089495.1	Clinical（Urine）	GCA_016503465.1	Environmental（NA）
GCF_000770605.1	Clinical（Bone culture）	GCF_023005135.1	Clinical（Urine）
GCF_030551235.1	Clinical（Tracheal secretion）	GCA_021387885.2	Clinical（Hospital ICU）
GCF_024461055.1	Environmental（NA）	GCF_022601755.1	Clinical（Tracheal aspirate）
GCF_005519135.2	Clinical（Cerebrospinal fluid）	GCF_037911775.1	Clinical（Sputum）
GCF_013372085.1	Environmental（Cell culture）	GCF_040595795.1	Clinical（Sputum）

长度≥50 bp、e值≤1×10^{-5}）对Prokka注释蛋白序列进行比对筛选IS[19]。

1.8　统计学方法

采用GraphPad Prism 8.0软件进行统计分析。数据采用均数加标准差表示。两组比较时，若数据服从正态分布且方差齐性，采用独立样本t检验。比较不同组生物膜形成能力（弱、中、强）的分布差异时，采用卡方检验，检验水准α=0.05。

2　结　果

2.1　细菌分布

共收集220株AB。其中临床感染组118株，环境来源组102株，环境分离率为18.1%（102/564）。临床感染组来源以痰液（42/118，35.6%）及支气管肺泡灌洗液（16/118，13.6%）为主。环境来源组来源呈多点定植特征。高频接触区及潮湿表面检出率显著，门把手、接待台面及垃圾桶盖分离率最高（33.3%），污物间及浴室地面分离率次之（25.0%）。

2.2　系统进化分析

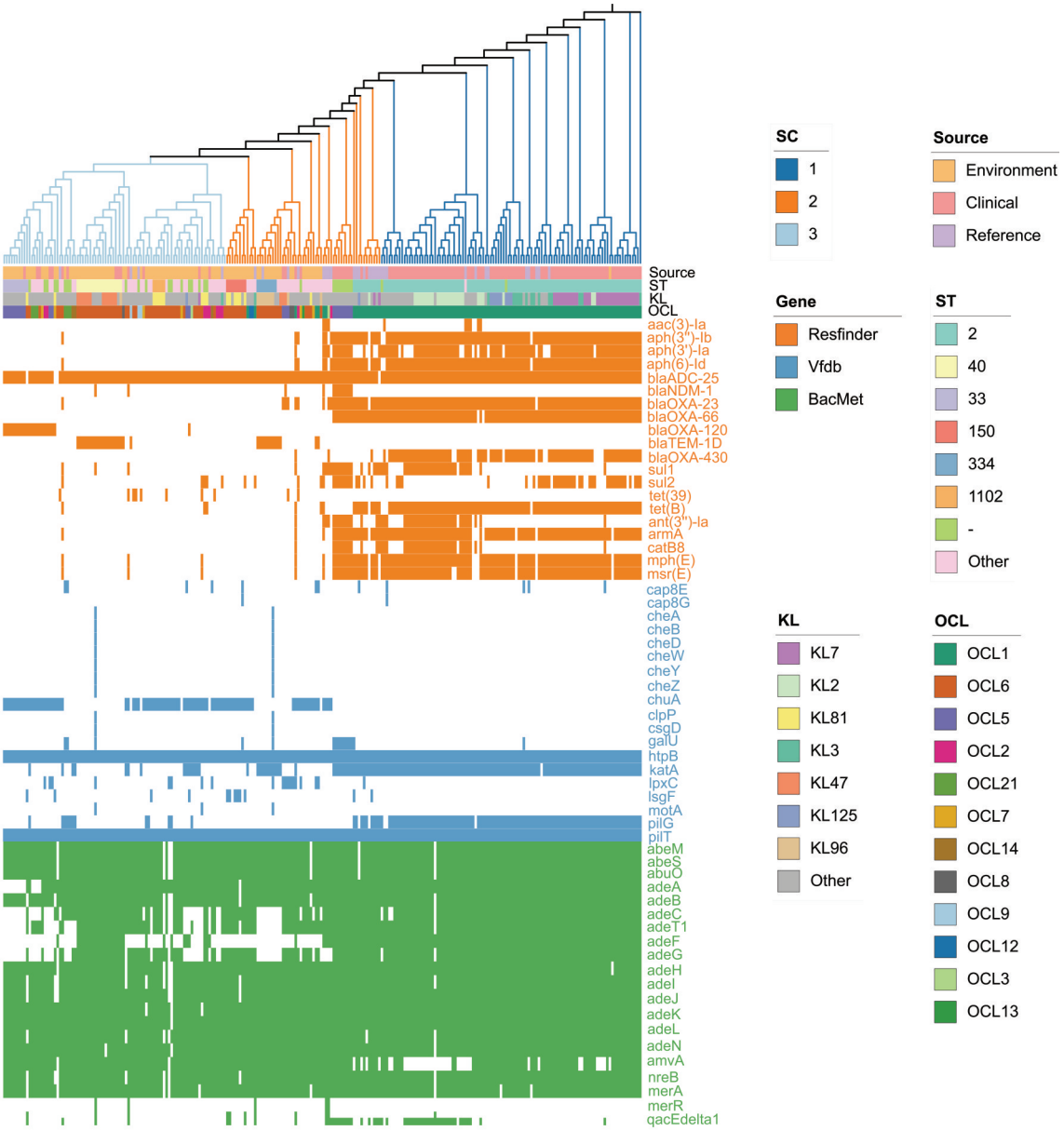
测序分析显示，220株AB分为38种已知ST型。ST2（92/220，41.82%）和ST40（18/220，8.18%）为优势谱系，荚膜型多为KL7及OCL1。进化分析显示聚集为SC1、SC2及SC3这3个克隆簇。其中SC1以临床感染组为主，而SC2和SC3以环境来源组和参考菌株组为主（图1）。

2.3　耐药表型与耐药谱

临床感染组整体耐药率较环境来源组高，其中MC、IMP、TOB、LVX等多数抗生素的耐药性显著高于环境来源组（P<0.001；图2）。耐药基因分析结果显示，$bla_{\mathrm{ADC-25}}$在两组中均高频检出，$bla_{\mathrm{OXA-23}}$、*aph(3")-Ib*及*tet*（B）等基因在临床株中检出率均超70%，显著高于环境来源组（P<0.001；图1）。

2.4　消毒剂耐受表型与基因

临床感染组对TCS和BAB的耐受能力显著高于环境来源组（图3）。基因层面，*adeJ*、*adeI*等基因在两组中检出率均高于95%。其中*adeH*、*adeG*、*adeB*等基因在临床感染组中显著富集（图1）。相关性分析显示，TCS与BAB的消毒剂耐药表型与MC、IMP、TOB等多种抗生素耐药表型呈显著正相关（P<0.05），如表2所示。



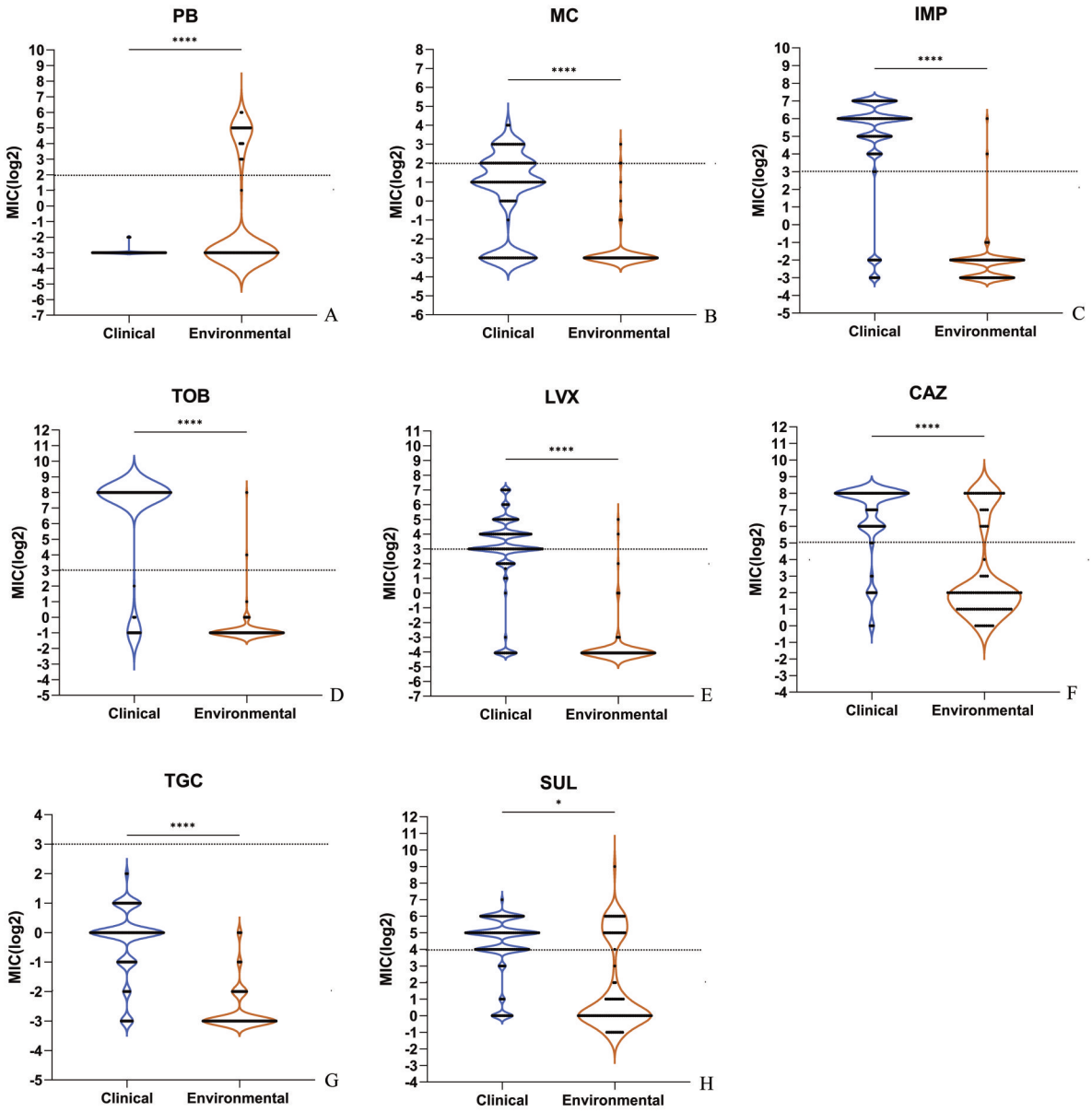
This tree was constructed based on core-genome SNPs of 220 local isolates and 32 reference genomes. Three distinct sequence clusters (SC1, SC2, and SC3) were identified, with SC1 predominantly consisting of clinical strains, while SC2 and SC3 were mainly composed of environmental isolates and reference genomes. For source information (clinical/environmental) of reference genomes, see Table 1. The colored columns on the right indicate Sequence Cluster (SC), Multilocus Sequence Type (ST), Capsular (KL) type, and O-antigen (OCL) type, respectively. Different colors represent distinct molecular lineages and origins. Gene annotations were performed using ResFinder (antimicrobial resistance genes), VFDB (virulence factors), and BacMet2 EXP (disinfectant resistance genes). Accordingly, the labels "ResFinder", "VFDB", and "BacMet" in the legend correspond to resistance, virulence, and disinfectant-related genes, respectively.

图1 252株鲍曼不动杆菌基因组系统发育树

Fig. 1 Whole-genome phylogenetic tree of 252 *A. baumannii*

2.5 毒力基因与生物膜形成能力

结晶紫染色法测定结果显示,根据生物膜形成能力将菌株分为弱成膜组(n=46)、中成膜组(n=94)和强成膜组(n=80)。环境来源组中强成膜菌株占比为64.7%(66/102),而临床感染组中强成膜菌株仅占11.9%(14/118);相反,临床感染组中弱成膜菌株占比为33.0%(39/118),高于环境来源组的6.9%(7/102)。两组间生物膜形成能力的分布差异具有统计学意义(χ^2=69.06, df=2, P<0.000 1, *Cramer's V*=0.560),提示环境来源组的生物膜形成



MICs were determined using the agar dilution method. A–H represent the MIC distributions of polymyxin B (PB), minocycline (MC), imipenem (IMP), tobramycin (TOB), levofloxacin (LVX), ceftazidime (CAZ), tigecycline (TGC), and sulbactam (SUL), respectively. The dotted lines indicate the resistance breakpoints; isolates positioned above these lines are classified as resistant. Breakpoints are defined according to the CLSI 2026 standards. Since there is currently no CLSI breakpoint for TGC against *A. baumannii*, the U.S. FDA breakpoint for Enterobacteriaceae was applied. Overall, the clinical infection group (n = 118) exhibited significantly higher MIC values than the environmental group (n = 102) for all tested agents (t = 2.209 to 20.77, all P < 0.05, except SUL P = 0.028 2). Detailed t and P values: PB (t = 5.931, P < 0.000 1); MC (t = 8.633, P < 0.000 1); IMP (t = 13.95, P < 0.000 1); TOB (t = 20.77, P < 0.000 1); LVX (t = 9.369, P < 0.000 1); CAZ (t = 8.083, P < 0.000 1); TGC (t = 12.82, P < 0.000 1); SUL (t = 2.209, P = 0.028 2).

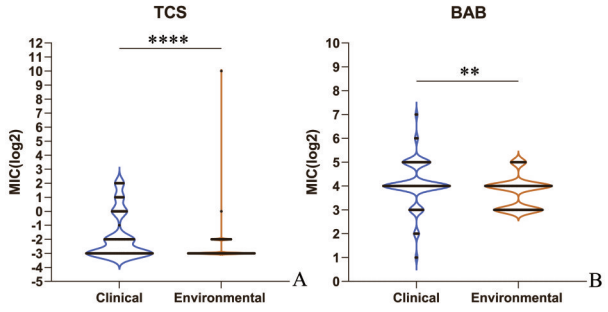
图2　不同来源鲍曼不动杆菌对8种抗菌药物的MIC分布

Fig. 2　Distribution of MICs of eight antimicrobial agents against *A. baumannii* from different sources

能力显著强于临床感染组（图4A–B）。生存曲线显示，强成膜组的致死作用高于中、弱成膜组（图4C）。毒力基因检出结果显示，*htpB*和*pilT*在两组中的检出率均为100%，*katA*、*pilG*和*clpP*等基因在临床感染组中的检出率更高（图1）。

2.6　质粒组学与IS特征分析

220株菌株共携带41种质粒谱系，其中如p1UC21460、p2VB33071等特定谱系共同携带多类抗性与毒力基因（图5）。经IS鉴定，共发现219种IS，优势家族为IS3（23.7%，52/219）、IS5（23.3%，51/



MICs were determined to evaluate the tolerance levels of clinical (n = 118) and environmental (n = 102) isolates to commonly used disinfectants. Panels A and B show the MIC distributions of triclosan (TCS) and benzalkonium bromide (BAB), respectively. The clinical infection group exhibited significantly higher tolerance to both TCS and BAB compared with the environmental group. Independent-samples t test results: TCS (t = 4.060, P < 0.000 1); BAB (t = 3.247, P = 0.001 4).

图3 鲍曼不动杆菌对2种消毒剂的最低抑菌浓度分布

Fig. 3 Distribution of MICs of two disinfectants against *A. baumannii*

219)及IS1(7.8%, 17/219)。IS1006、IS1007和ISVsa3与bla_{OXA-23}、*aph(3")-Ib*、*aph(6)-Id*等耐药基因高频共现;IS1006、IS1007、IS1008、ISAba52等IS与*katA*等关键毒力基因频繁共现,IS15、ISAba21、ISAcsp12等IS与*adeB*、*abeS*等消毒剂耐药基因在临床感染组中表现出高频共现特征。

3 讨论

AB感染与ICU患者的高病死率密切相关[20],了解其在院内的流行现状及基因组特征是感染防控的核心。本研究对220株临床以及医院环境来源AB的分子流行病学分析显示,ST2为本院绝对优势流行克隆,这与国际报道中ST2作为全球多重耐药优势谱系的结论一致[21]。

AB的耐药性与其携带的耐药基因高度相关。本研究中临床感染组的MIC值及耐药基因丰富度(如bla_{OXA-23}、*armA*及*tet(B)*)相较于环境来源组均表现出显著优势,提示临床压力下菌株具有更强的抗生素选择适应性。值得注意的是,尽管环境来源组多重耐药率较低,但$bla_{OXA-430}$等特定耐药基因的检出率反而高于临床感染组。这一现象表明,医院环境不仅是耐药菌的储存地,更是耐药基因演化与传播的潜在源头[22]。

除常规抗生素外,AB对消毒剂的耐受性也不容忽视。已有研究表明,外排泵系统的激活是AB减少胞内消毒剂聚集、提升耐受水平的核心机制之一[23]。本研究发现临床感染组对TCS和BAB的耐受能力显著强于环境来源组,且显著富集了*adeN*、*adeB*及*qacEΔ1*等外排泵相关基因。这一表型与基因型的关联暗示,这种耐受性的提高或许与临床环境下长期消毒带来的压力密切相关[24],这些外排泵及其调控机制使AB能在医院环境中抵御消毒剂作用并在环境表面存活,进一步增加了其传播风险[25]。

生物膜的形成能力是决定AB环境耐受与致病性的关键。已有研究表明临床来源菌株普遍表现出更强的生物膜形成能力和毒力基因富集特征,进而增强了其在医院环境中的持久生存能力和其在呼吸机相关肺炎、血流感染及手术部位感染的发生风险[26]。本研究中,环境来源组的强成膜菌株比例显著高于临床感染组;此外,大蜡螟感染实验进一步证实,生物膜成膜能力与体内致死率呈正相关。这一结果提示,具备强成膜能力的AB具有更高的毒力水平。这很可能是导致临床感染高发、病情反复及治疗难度增加的核心因素[27]。

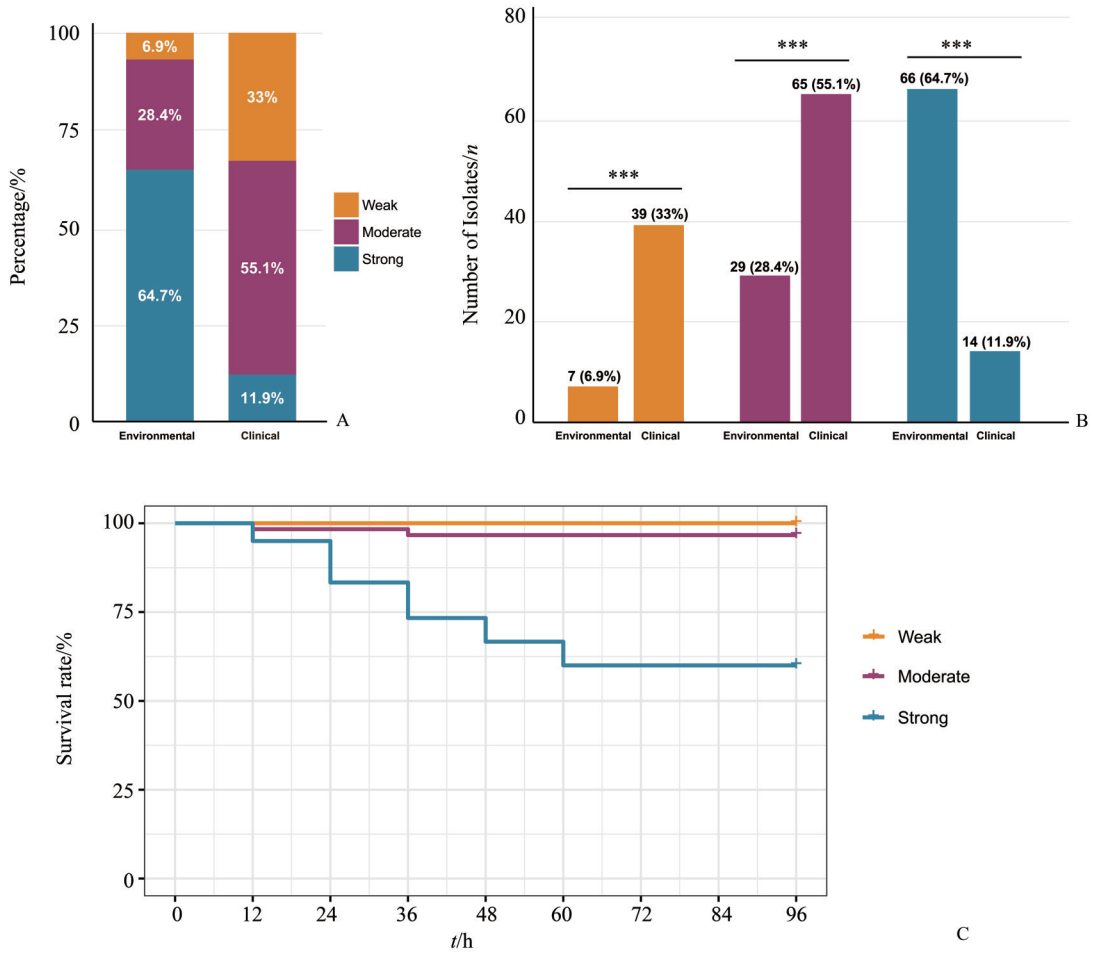
IS介导了耐药与毒力基因的水平转移,进而增

表2 消毒剂MIC与抗生素MIC的Spearman相关性分析

Table 2 Spearman correlation analysis between disinfectant MICs and antibiotic MICs

	PB	MC	IMP	TOB	LVX	CAZ	TGC	SUL
TCS	−0.079	+0.227*	+0.252*	+0.269*	+0.205*	+0.178*	+0.282*	+0.225*
BAB	−0.063	+0.339*	+0.343*	+0.360*	+0.357*	+0.228*	+0.381*	+0.285*

Spearman correlation analysis was used to assess the relationship between phenotypic tolerance to disinfectants (TCS and BAB) and resistance to various antimicrobial agents. "+" indicates a positive correlation (r_s>0); "−" indicates a negative correlation (r_s<0); "*" indicates a statistically significant correlation (P<0.05). Significant positive correlations were observed between disinfectant tolerance (TCS and BAB) and resistance phenotypes for multiple antibiotics, including MC, IMP, and TOB (P<0.05). All correlation analyses were based on n = 220 isolates (clinical n = 118, environmental n = 102).



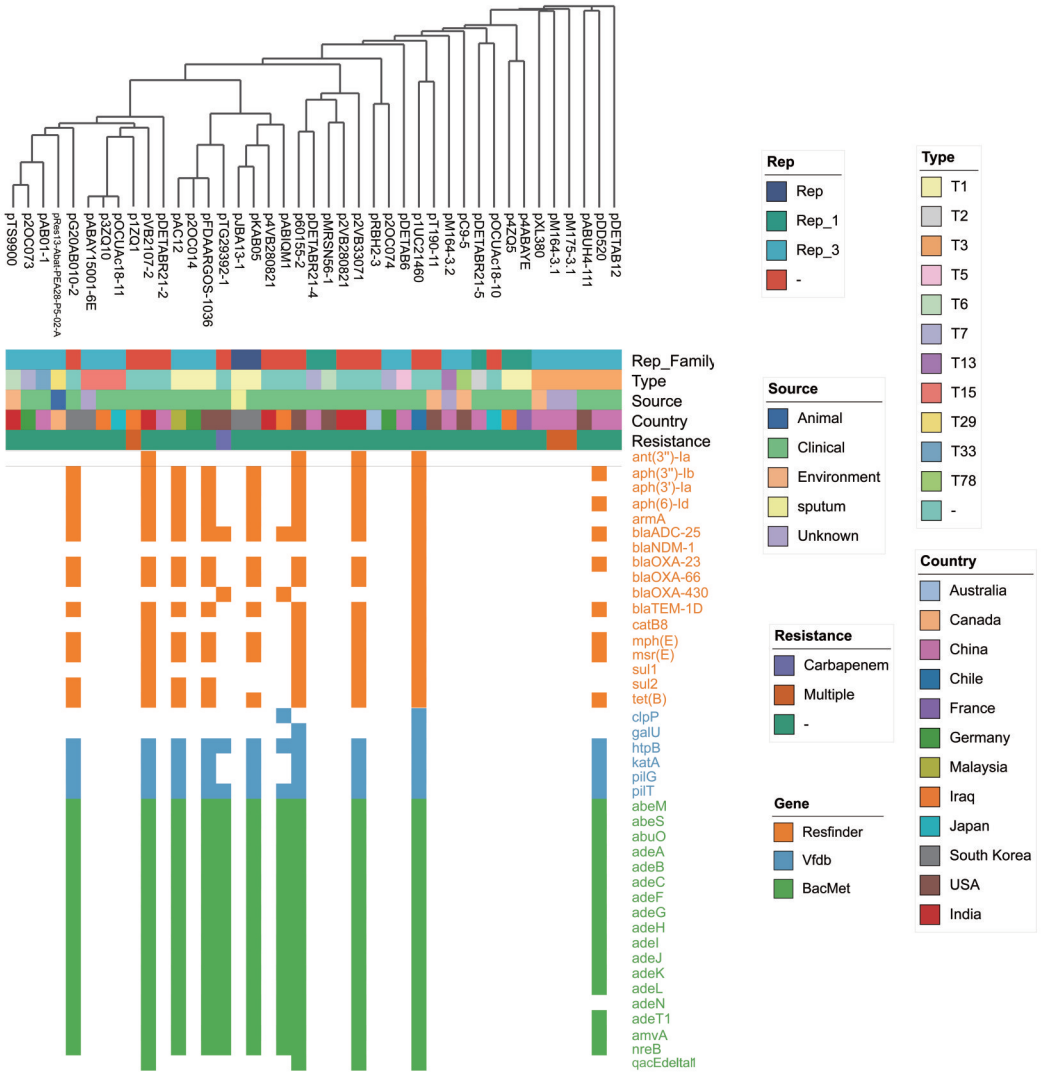
Biofilm formation was quantified using the crystal violet staining method. Panel A shows the distribution of biofilm-forming capacity among isolates, with numbers on the bars representing percentages. Panel B compares the proportion of clinical and environmental isolates across different biofilm categories. The environmental group showed a significantly higher proportion of strong biofilm producers (64.7%, 66/102) compared with the clinical infection group (11.9%, 14/118). Statistical significance was determined using the Chi-square test (χ^2=69.06, *df*=2, $^{***}P < 0.000\ 1$), and the effect size was measured by *Cramer's V* (0.560). Panel C displays the survival curves of *Galleria mellonella* larvae infected with *A. baumannii* strains of varying biofilm strengths. The lethal effect of the strong biofilm group was significantly higher than that of the moderate and weak groups. Survival curves were compared using the Log-rank (Mantel-Cox) test.

图4　鲍曼不动杆菌生物膜形成能力分布与生存曲线分析

Fig. 4　Distribution of biofilm formation ability and survival curve analysis of *A. baumannii*

强了菌株的耐药性和适应能力[28]。本研究发现，多种IS与消毒剂耐受基因及毒力基因密切相关，表明其可能参与调控或促进这些关键基因的水平转移。p1UC21460等质粒与耐药基因及毒力基因的高频共现，进一步阐明了这些质粒在传播耐药性、致病性和环境适应性相关基因中的关键作用[29]。未来研究需通过多中心前瞻性设计弥补单中心样本的不足，以动态追踪菌株进化轨迹；同时，有待结合三代测序与接合实验，深入阐明相关遗传元件的水平转移机制。

本研究系统评价了院内感染及环境来源AB的分子流行病学特征，解析了耐药、毒力及消毒剂耐受表型在不同来源菌株间的分布差异，并展示了耐药与毒力基因在遗传元件上的共现情况。研究提示，当前院内及环境中的优势克隆株防控形势依然严峻。临床应采取综合干预措施，包括落实抗生素分级管理、规范环境消毒流程以及阻断院内传播路径，以有效遏制多重耐药菌的流行，最终改善患者临床预后。



This phylogenetic tree represents the diversity of 41 distinct plasmid lineages identified among 220 *A. baumannii* isolates. Specific lineages, such as p1UC21460 and p2VB33071, were found to co-carry multiple classes of antimicrobial resistance (AMR) genes and virulence factors. The annotation columns on the right represent: Rep, plasmid replicon family; Source, origin of the plasmid; Resistance, antimicrobial resistance genes carried by the plasmid; Type, molecular classification of the plasmid; Country, geographical origin; and Gene, other functional genes identified. Different colors indicate distinct categories within each metadata column.

图5 鲍曼不动杆菌质粒进化树

Fig.5 Plasmid phylogenetic tree of *A. baumannii*

参考文献

[1] Najafabadi MK, Soltani R. Carbapenem-resistant *Acinetobacter baumannii* and ventilator-associated pneumonia: epidemiology, risk factors, and current therapeutic approaches [J]. J Res Pharm Pract, 2024, 13(2): 33-40.

[2] Gao J, Zou Y, Wang Y, et al. Breath analysis for noninvasively differentiating *Acinetobacter baumannii* ventilator-associated pneumonia from its respiratory tract colonization of ventilated patients [J]. J Breath Res, 2016, 10(2):1752-7155.

[3] Monem S, Furmanek-Blaszk B, Łupkowska A, et al. Mechanisms protecting *Acinetobacter baumannii* against multiple stresses triggered by the host immune response, antibiotics and outside-host environment [J]. Int J Mol Sci, 2020, 21(15): 1-20.

[4] Vital M, Woltemate S, Schlüter D, et al. Molecular epidemiology, microbiological features and infection control strategies for carbapenem-resistant *Acinetobacter baumannii* in a German

burn and plastic surgery center (2020-2022) [J]. Antimicrob Resist Infect Control, 2024, 13(1):99-105.
[5] 白雪皎, 胡雪姣, 赵越, 等. 广泛耐药鲍曼不动杆菌肺部感染的危险因素分析[J]. 新医学, 2023, 54(2): 140-143.
Bai XJ, Hu XJ, Zhao Y, et al. Analysis of risk factors for pulmonary infection caused by extensively drug-resistant *Acinetobacter baumannii*[J]. J New Med, 2023, 54(2): 140-143.
[6] Tascini C, Giuliano S, Martini L, et al. OXA-carbapenemases and mutations within PBPs in ST2 carbapenem-resistant A. *baumannii*: evaluating the efficacy of cefiderocol and ampicillin-sulbactam combination therapy [J]. J Glob Antimicrob Resist, 2025, 44: 189-196.
[7] Valcek A, Nesporova K, Whiteway C, et al. Genomic analysis of a strain collection containing multidrug- , extensively drug- , pandrug- , and carbapenem-resistant modern clinical isolates of *Acinetobacter baumannii* [J]. Antimicrob Agents Chemother, 2022, 66(9): e0089222.
[8] Shimose LA, Masuda E, Sfeir M, et al. Carbapenem-resistant *Acinetobacter baumannii*: concomitant contamination of air and environmental surfaces [J]. Infect Control Hosp Epidemiol, 2016, 37(7): 777-781.
[9] Wong SC, Lam GK, Chen JH, et al. Air dispersal of multidrug-resistant *Acinetobacter baumannii*: implications for nosocomial transmission during the COVID-19 pandemic [J]. J Hosp Infect, 2021, 116: 78-86.
[10] Havenga B, Reyneke B, Ndlovu T, et al. Genotypic and phenotypic comparison of clinical and environmental *Acinetobacter baumannii* strains [J]. Microb Pathog, 2022, 172: 105749.
[11] Cameranesi MM, Paganini J, Limansky AS, et al. Acquisition of plasmids conferring carbapenem and aminoglycoside resistance and loss of surface-exposed macromolecule structures as strategies for the adaptation of *Acinetobacter baumannii* CC104(O)/CC15(P) strains to the clinical setting [J]. Microb Genom, 2020, 6(9):mgen000360.
[12] Schuetz AN, Ferrell A, Hindler JA, et al. Overview of changes in the clinical and laboratory standards institute performance standards for antimicrobial susceptibility testing: M100 32nd and 33rd editions [J]. J Clin Microbiol, 2025, 63(9): e0162323.
[13] Stepanović S, Vuković D, Hola V, et al. Quantification of biofilm in microtiter plates: overview of testing conditions and practical recommendations for assessment of biofilm production by staphylococci [J]. APMIS, 2007, 115(8): 891-899.
[14] Muzahid NH, Ramesh A, Siew TH, et al. Comparison of the virulence of community- and hospital- isolated *Acinetobacter baumannii* in HeLa cell line and insect model, Galleria mellonella [J]. Access Microbiol, 2025, 7(2):000858.v3.
[15] Papp M, Solymosi N. Review and comparison of antimicrobial resistance gene databases [J]. Antibiotics (Basel), 2022, 11(3):1169-1174.
[16] Wyres KL, Cahill SM, Holt KE, et al. Identification of *Acinetobacter baumannii* loci for capsular polysaccharide (KL) and lipooligosaccharide outer core (OCL) synthesis in genome assemblies using curated reference databases compatible with Kaptive [J]. Microb Genom, 2020, 6(3):e000339.
[17] Didelot X, Wilson DJ. ClonalFrameML: efficient inference of recombination in whole bacterial genomes [J]. PLoS Comput Biol, 2015, 11(2): e1004041.
[18] Tobin LA, Lam MMC, Hamidian M. Pan-genus analysis and typing of antimicrobial resistance plasmids in *Acinetobacter* [J]. NPJ Antimicrob Resist, 2025, 3(1): 65-70.
[19] Siguier P, Perochon J, Lestrade L, et al. ISfinder: the reference centre for bacterial insertion sequences [J]. Nucleic Acids Res, 2006, 34(Database issue): 32-36.
[20] Kurihara MNL, Sales RO, Silva KED, et al. Multidrug-resistant *Acinetobacter baumannii* outbreaks: a global problem in healthcare settings [J]. Rev Soc Bras Med Trop, 2020, 53: e20200248.
[21] Pearl S, Anbarasu A. Genomic landscape of nosocomial *Acinetobacter baumannii*: a comprehensive analysis of the resistome, virulome, and mobilome [J]. Sci Rep, 2025, 15(1): 18203.
[22] Fahy S, O'Connor JA, Lucey B, et al. Hospital reservoirs of multidrug resistant *Acinetobacter* species-the elephant in the room! [J]. Br J Biomed Sci, 2023, 80: 11098.
[23] Lin F, Xu Y, Chang Y, et al. Molecular characterization of reduced susceptibility to biocides in clinical isolates of *Acinetobacter baumannii* [J]. Front Microbiol, 2017, 8: 1836.
[24] Milani ES, Hasani A, Varschochi M, et al. Biocide resistance in *Acinetobacter baumannii*: appraising the mechanisms [J]. J Hosp Infect, 2024, 154: 122-123.
[25] Pallós P, Gajdács M, Urbán E, et al. Characterization of antibiotic and disinfectant susceptibility in biofilm-forming *Acinetobacter baumannii*: a focus on environmental isolates [J]. Eur J Microbiol Immunol (Bp), 2024, 14(2): 126-133.
[26] Rajangam SL, Narasimhan MK. Current treatment strategies for targeting virulence factors and biofilm formation in *Acinetobacter baumannii* [J]. Future Microbiol, 2024, 19(10): 941-961.
[27] Lucidi M, Visaggio D, Migliaccio A, et al. Pathogenicity and virulence of *Acinetobacter baumannii*: factors contributing to the fitness in healthcare settings and the infected host [J]. Virulence, 2024, 15(1): 2289769.
[28] Partridge SR, Kwong SM, Firth N, et al. Mobile genetic elements associated with antimicrobial resistance [J]. Clin Microbiol Rev, 2018, 31(4):e00088-17.
[29] Feng Z, Wang L, Guan Q, et al. *Acinetobacter baumannii* coordinates central metabolism, plasmid dissemination, and virulence by sensing nutrient availability [J]. mBio, 2023, 14(6): e0227623.

(编辑　孙慧兰)